methods were used for this purpose. The single imaginary vibrational frequency is predicted to be 1166i cm^{-1} (DZ SCF) and 1267i cm^{-1} (DZP SCF), and the corresponding normal mode vibrational eigenvector does indeed connect the transition state to the HCN + HCN + N_2 products.

More reliable estimates of the classical barrier height for the triple dissociation were obtained from configuration interaction (CI) wave functions including all single and double excitations. For the larger DZP basis set the correlated wave functions involved a total of 187 526 configurations. The effects of higher excitations were estimated via Davidson's correction[17] for unlinked clusters. A more reliable treatment of unlinked clusters is provided by the coupled cluster single and double excitation (CCSD) method.[18]

The present energetic predictions are summarized in Table I. At the highest level of theory, CCSD with zero-point vibrational energies appended, the activation energy for reaction 2a is predicted to be (52.8 - 5.8) = 47.0 kcal/mol. This prediction is 4.8 kcal/mol lower than the experimental upper limit. However, it is well established[13b,19] that such levels of theory yield activation energies above available observed E_a values, and an estimate of the expected error might be 3 kcal/mol. Thus we conclude that the unimolecular triple dissociation proceeds with an energy below the $S_0 \rightarrow S_1$ electronic excitation energy of *s*-tetrazine.

Acknowledgment. This research was supported by the U.S. National Science Foundation, Division of Chemistry, Chemical Physics Program, Grant CHE-821875. We thank Professor C. Bradley Moore for helpful discussions.

(17) Davidson, E. R. *The World of Quantum Chemistry*; Daudel, R., Pullman, B., Eds.; D. Reidel: Dordrecht, Holland, 1974; pp 17-30.
(18) Purvis, G. D.; Bartlett, R. J. *J. Chem. Phys.* **1982**, *76*, 1910.
(19) Schaefer, H. F. *J. Phys. Chem.* **1985**, *89*, 5336.

Diffusion-Controlled Association Rate of Cytochrome *c* and Cytochrome *c* Peroxidase in a Simple Electrostatic Model

Scott H. Northrup,* John C. L. Reynolds, Cynthia M. Miller, Kristi J. Forrest, and Jeffrey O. Boles

Contribution from the Department of Chemistry, Tennessee Technological University, Cookeville, Tennessee 38505. *Received June 30, 1986*

Abstract: The diffusion-controlled association of electron transport proteins cytochrome *c* and cytochrome *c* peroxidase is simulated by the Brownian Dynamics method. The proteins are modelled as spheres, each having a central monopole carrying the net charge and two dipolar charges imbedded 1.0 Å inside the protein surface. The magnitudes of the monopole and dipole moments generated by this simplified charge distribution are determined directly from the X-ray crystallographic coordinates of the proteins by assigning partial charges to each non-hydrogen atom. Solvent electrolyte effects are modelled by using the Debye-Hückel screening law modified to include the effect of the large ion-exclusion sizes of macromolecules. Rate constants obtained by the simulation compare moderately well with experimentally determined rate constants for electron transfer at physiological ionic strength. The electrostatic torques generated by inclusion of the dipolar terms in the interaction potential are of crucial importance in overcoming the severe rate-retarding effect of the orientational reactivity constraints. At lower ionic strengths, dissociation rather than diffusion-controlled association is rate limiting for this particular reaction. The computed ionic strength dependence of the rate constant is weaker than that observed in the experiment, presumably because of the failure of the Debye-Hückel screened Coulombic potential to adequately treat solvent mediation effects as ionic strength increases. Simulation results are sensitive to the mode of treatment of the solvent mediation effects and choice of effective protein radii.

I. Introduction

The rates of many important biological processes in solution are influenced or controlled by the diffusional encounter rate of reactants.[1] Important examples include the bimolecular reaction of enzymes and ligands, antibodies and antigens, hormones and receptors, electron transport protein association, and sliding of small molecules on DNA. Molecular recognition in biochemical reactions not only depends on static conformational properties of biomolecules obtainable by X-ray diffraction data, but it may depend on dynamics as well. It has already been argued[2] that molecular specificity may in fact begin in the diffusional encounter stage of the reaction, with long-ranged electrostatic forces and other factors selectively steering particles into favorable orientations for reaction. In this paper we examine the role played by electrostatic structural features in the diffusion-controlled association rate of electron-transport proteins cytochrome *c* and cytochrome *c* peroxidase.

A number of important theoretical studies have addressed the problem of calculating the rate of diffusion-controlled reactions between macromolecules.[3] Smoluchowski and Debye investigated the problem of diffusion-controlled reactions between uniformly reactive spheres in the absence[4] and presence[5] of centrosymmetric Coulombic forces. Since these pioneering works, there has been a proliferation of theoretical studies based on more refined models. In many types of important problems analytical solutions have been obtained for rate constants. Unfortunately, one cannot hope to obtain analytical solutions on the detailed level required to understand molecular recognition in biomolecular interactions in general when a variety of interactions operate simultaneously. For this reason one must resort to numerical methods. A computer simulation approach based on the Brownian Dynamics (BD) trajectory method has been developed[6] to handle the arbitrarily

* Author to whom correspondence should be addressed.

(1) McCammon, J. A.; Harvey, S. C. *Dynamics of Proteins and Nucleic Acids*; Cambridge University Press: London; in press.
(2) Neumann, E. In *Structural and Functional Aspects of Enzyme Catalysis*; Eggerer, H., Huber, R., Eds.; Springer-Verlag: Berlin-Heidelberg-New York, 1981.
(3) Berg, O. G.; Hippel, P. H. von *Annu. Rev. Biophys. Biophys. Chem.* **1985**, *14*, 131.
(4) Smoluchowski, M. V. *Phys. Z.* **1916**, *17*, 557.
(5) Debye, P. *Trans. Electrochem. Soc.* **1942**, *82*, 265.
(6) Northrup, S. H.; Allison, S. A.; McCammon, J. A. *J. Chem. Phys.* **1984**, *80*, 1517.

0002-7863/86/1508-8162$01.50/0

complicated interactions present in real biophysical systems. In this approach the Brownian motion of interacting macromolecules is simulated stochastically by a series of small displacements chosen from a distribution which is equivalent to the short time solution of the diffusion equation.[7-9] Diffusion-influenced bimolecular reaction rate constants may then be extracted from collision probabilities calculated from a large number of BD trajectories.[6] The ease of implementation of this method has been demonstrated in the case of model reactions with hydrodynamic interactions, chemically anisotropic species, rotational diffusion, and various intermolecular force models.[10-15]

The BD method has been successfully applied[12,13,16,17] to calculations of the electrostatic effects in the diffusion-controlled reaction of the enzyme superoxide dismutase (SOD) with its substrate O_2^-. In that study the SOD dimer was modelled as a sphere of radius 30 Å having 2 reactive patches corresponding to active site regions. A five charge model was used to reproduce the monopole, dipole, and quadrupole terms associated with the charged groups in the 2.0 Å resolution X-ray structure of bovine erythrocyte SOD. It was determined that the electrostatic quadrupole increases the reaction rate by 40% by steering the substrate into the active site region. This effect essentially overcomes the retarding effect of the repulsive interaction between two species having net negative charges. Similar results were obtained from a more detailed 2196-charge model of SOD.[12]

In this paper the BD method is applied to the calculation of the diffusion-controlled association rate between the electron-transport proteins cytochrome *c* and cytochrome *c* peroxidase, a system chosen because the kinetics are well-studied experimentally[18] and because of the anticipated dominance of electrostatic features of the proteins in their biological function.[19] This offers a unique opportunity to understand the relationship between protein structural features and electron-transport process in particular, and to assess the role of electrostatic effects in the diffusion-controlled reactions of biomolecules in a more quantitative fashion in general.

The electron-transfer reaction between cytochrome *c* and cytochrome *c* peroxidase has been widely studied as an important prototypical model for understanding heme-catalyzed reductive cleavage of O–O bonds and the coupling of this event to electron transfer in the electron-transport chain.[20] A tentative conclusion of these experimental studies is that cytochrome *c* has a functionally significant dipole moment vector ($\simeq$300 D), the positive end of which passes through the electron-transfer surface.[21] This may act as a steering device to enhance a very orientation-dependent reaction with negatively charged physiological reaction partners long before they reach juxtaposition. It has been shown by X-ray diffraction studies and computer graphics[22] that a high degree of complementarity exists between negatively charged aspartates on the peroxidase and positively charged lysines on cytochrome *c* lining the electron-transfer site. The relative importance (to the dynamics) of the detailed charge configuration around the electron-transfer surface vs. the effect of the net monopole and dipole interactions of the molecule remains to be shown. In addition to understanding electrostatic influences in diffusion-controlled reactions, these studies give us a unique opportunity to quantitatively compare theoretical and experimental results for diffusion-influenced reactions in which structural features of the reactive macromolecules are well-characterized.

In section II we calculate the electrostatic properties of horse cytochrome *c* and yeast cytochrome *c* peroxidase by using available X-ray diffraction data. A simple electrostatic model of the protein–protein interaction potential is developed for the purpose of BD simulation. In addition to the input of electrostatic parameters, estimates are made of the diameters, transport coefficients, and reactive patch sizes that are appropriate to model cytochrome *c* and cytochrome *c* peroxidase, and a simple treatment of ionic strength effects is discussed. In section III we present the results of the BD simulation and compare our rate constants with experiment, and in section IV we give a summary and concluding remarks.

II. Models and Procedure

A. Electrostatic Model of Cytochrome *c* and Cytochrome *c* Peroxidase. The electrostatic properties of the proteins horse ferrocytochrome *c* (CYTC) and yeast cytochrome *c* peroxidase (CYP) were calculated from all-atom coordinate sets available through the Protein Data Bank.[23] The horse CYTC conformation was calculated by mutational extension of the 1.5 Å resolution tuna CYTC X-ray crystallographic structure.[24] All side chain atoms of the 18 amino acid residues in horse CYTC which differ from those of the tuna protein[25] were fitted onto the tuna backbone without energy refinement by using standard residue coordinates in the GROMOS package.[26] Since the tuna protein has no carboxy-terminal residue 104, the horse residue Glu-104 backbone was extended from the Asp-103 backbone by using backbone angles ($\psi_{103},\omega_{103},\phi_{104},\psi_{104}$) = (180°,180°,180°,180°). The coordinates of yeast CYP were taken from the 1.7 Å resolution X-ray crystallographic structure contributed by Finzel, Poulos, and Kraut.[27] The 68 surface side chain atoms missing from this set because of excessive motional disorder in the crystal were fitted into the structure by using standard residue coordinates as described above. In addition, the seven heavy atoms of the entire Thr-1 backbone and side chain (missing due to motional disorder) were built onto Thr-2 by using backbone dihedral angles (ϕ_2,ψ_1,ω_1) = (180°,180°,180°) for residue 1.

The net protein charge and dipole orientation and magnitude for both proteins were computed by assigning partial charges to *each* atom in the protein according to partial charge values computed by a CNDO/2 semiempirical quantum calculation on individual amino acid and heme units.[28] For the most accurate electrostatic model at a neutral pH it is assumed that in both proteins all lysines and arginines are protonated, and the aspartic, glutamic, and carboxy-terminal acid groups are dissociated.[29] The heme propionate side chains in both proteins are assumed to be undissociated[30-32] in the best model. Our model differs from the

(7) Ermak, D. L.; McCammon, J. A. *J. Chem. Phys.* **1978**, *69*, 1352.
(8) Turq, P.; Lantelme, F.; Friedman, H. L. *J. Chem. Phys.* **1977**, *66*, 3039.
(9) Fixman, M. *J. Chem. Phys.* **1978**, *69*, 1527, 1538.
(10) Allison, S. A.; Northrup, S. H.; McCammon, J. A. *J. Chem. Phys.* **1985**, *83*, 2894.
(11) Northrup, S. H.; Curvin, M.; Allison, S. A.; McCammon, J. A. *J. Chem. Phys.* **1986**, *84*, 2196.
(12) Ganti, G.; McCammon, J. A.; Allison, S. A. *J. Phys. Chem.* **1985**, *89*, 3899.
(13) Allison, S. A.; McCammon, J. A.; Northrup, S. H. In *Coulombic Interactions in Macromolecular Systems*"; ACS Symposium Series 302; American Chemical Society: Washington, DC, 1986; p 216.
(14) Northrup, S. H.; Smith, J. D.; Boles, J. O.; Reynolds, J. C. L. *J. Chem. Phys.* **1986**, *84*, 5536.
(15) McCammon, J. A.; Northrup, S. H.; Allison, S. A., *J. Phys. Chem.* **1986**, *90*, 3901.
(16) Allison, S. A.; Ganti, G.; McCammon, J. A. *Biopolymers* **1985**, *24*, 1323.
(17) Allison, S. A.; McCammon, J. A. *J. Phys. Chem.* **1985**, *89*, 1072.
(18) Kang, C. H.; Brautigan, D. L.; Osheroff, N.; Margoliash, E. *J. Biol. Chem.* **1978**, *253*, 6502.
(19) Margoliash, E.; Bosshard, H. R. *Trends Biochem. Sci.* **1983**, *8*, 316.
(20) Kraut, J. *Biochem. Soc. Trans.* **1981**, *9*, 197.
(21) Koppenol, W. H.; Margoliash, E. *J. Biol. Chem.* **1982**, *257*, 4426.
(22) Poulos, T. L.; Kraul, J. *J. Biol. Chem.* **1980**, *255*, 10322. (These authors mistakenly refer to Asn-216 as Asp-216.)
(23) Bernstein, F. C.; Koetzle, T. F.; Williams, G. J. B.; Meyer, E. F., Jr.; Brice, M. D.; Rodgers, J. R.; Kennard, O.; Shimanouchi, T.; Tasumi, M. *J. Mol. Biol.* **1977**, *112*, 535.
(24) Takano, T.; Dickerson, R. E. *Proc. Natl. Acad. Sci. U.S.A.* **1980**, *77*, 6371.
(25) Dickerson, R. E.; Takano, T.; Eisenberg, D.; Kallai, O. B.; Samson, L.; Cooper, A.; Margoliash, E. *J. Biol. Chem.* **1971**, *246*, 1511.
(26) Berendsen, H. J. C.; Postma, J. P. M.; Gunsteren, W. F. van; Hermans, J. In *Intermolecular Forces*; Pullman, B., Ed.; Reidel: Dordrecht, Holland, 1981; p 331.
(27) Finzel, B. C.; Poulos, T. L.; Kraut, J. *J. Biol. Chem.* **1984**, *259*, 13027.
(28) See Table AIII of McCammon (McCammon, J. A.; Wolynes, P. G.; Karplus, M., *Biochemistry*, 1979, *18*, 927) and Table 12 of Northrup (Northrup, S. H.; Pear, M. R.; Morgan, J. D.; McCammon, J. A.; Karplus, M. *J. Mol. Biol.* **1981**, *153*, 1087).
(29) Matthew, J. B. *Annu. Rev. Biophys. Biophys. Chem.* **1985**, *14*, 387.
(30) Takano, T.; Trus, B. L.; Mandel, N.; Mandel, G.; Kallai, O. B.; Swanson, R.; Dickerson, R. E. *J. Biol. Chem.* **1977**, *252*, 776.

Table I. Comparison of Electrostatic Properties of Several Models of Horse CYTC

horse ferrocytochrome *c* model	heme propionates charged	helix simple dipole treatment	q^a	$\|\mu\|^b$	η^c	ca. pt. at which (+) end of dipole vector crosses protein surface	
all-atom partial	no	N/A	8	286	0	$C_{\delta 1}$	Ile-81
charge model	yes	N/A	6	245	16	$C_{\delta 2}$	Ile-81
formal charge at	no	yes	8	274	5	C	Met-80
actual side	yes	yes	6	238	20	N	Phe-82
chain location	no	no	8	305	4	C_α	Met-80
	yes	no	6	259	12	C_β	Ile-81
net residue	no	yes	8	292	2	C_α	Met-80
charge at C_α	yes	yes	6	247	13	C_α	Ile-81
location	no	no	8	327	10	O	Lys-79
	yes	no	6	276	10	N	Ile-81
formal charge	no	yes	8	308	30	C_β	Phe-82
model at actual side chain location (Koppenol and Margoliash)	no	no	8	345	16	$C_{\delta 2}$	Ile-81

$^a q$ = net charge. $^b |\mu|$ = dipole magnitude (D). $^c \eta$ = dipole vector angle relative to "best model".

Table II. Comparison of Electrostatic Properties of Various Models of Yeast CYP

cytochrome *c* peroxidase	heme propionates charged	helix simple dipole treatment	q^a	$\|\mu\|^b$	η^c	ca. pt. where (−) end of dipole vector crosses protein surface	
all-atom partial	no	N/A	−12	425	0	O	Gly-178
charge model	yes	N/A	−14	520	7	C	Gly-178
formal charge at	no	yes	−12	486	5	C	Gly-178
actual side	yes	yes	−14	584	10	N	Lys-179
chain location	no	no	−12	416	6	C	Gly-178
	yes	no	−14	515	12	C_δ	Lys-179
net residue	no	yes	−12	489	15	C_δ	Pro-190
charge at C_α	yes	yes	−14	587	16	C	Gly-189
location	no	no	−12	426	19	N	Pro-190
	yes	no	−14	524	20	C_α	Gly-189

$^a q$ = net charge. $^b |\mu|$ = dipole magnitude (D). $^c \eta$ = dipole vector angle relative to "best model".

electrostatic model of Koppenol and Margoliash[21] used for CYTC in that they assign charges only to formally charged atoms and not to every atom. Peptide bond dipoles, which contribute to the global electrostatic properties mainly through α-helix region alignment, are treated approximately in their work by placing $+1/2e$ and $-1/2e$ charges at the nitrogen and carboxy terminal sides of α-helices, respectively, according to a procedure of Hol.[33] This is unncessary in our most accurate models because of the all-atom treatment.

The dipole moments of the proteins are computed by the equations given in the supplementary section of ref 21 for macromolecules with net charge. Comparisons of the dipole magnitudes and orientations for electrostatic models of various detail are displayed in Tables I and II, and in the case of horse CYTC a comparison is made with ref 21. First, note that both proteins are highly charged species and of opposite sign, +8e and −12e for CYTC and CYP when heme propionate carboxyl groups are undissociated. In subsequent BD simulations we will confirm that the large Coulombic attractive force between these species is necessary to provide for the large association rate constant observed in experiment, as well as the negative slope of the Brønsted–Bjerrum plot of the log of the rate constant vs. square root of the ionic strength. However, it will be apparent from BD simulation results that the net charge alone does not enhance the association rate sufficiently to offset the retarding effect of the orientational constraints for electron transfer. Additional significant electrostatic factors in this reaction are the large dipole moments on both proteins. This has already been documented for horse CYTC as perhaps playing a major factor in the facility of electron-transfer reactions of CYTC with its redox partners.[19] Our best electrostatic model for CYTC (see Table I) yields a dipole moment magnitude of 286 D, with the positive end passing through surface atom $C_{\delta 1}$ of Ile-81. In the center of mass reference frame, the dipole vector makes only a 27° angle with the position vector of surface heme atom CH_δ at the center of the exposed heme edge where electron transfer to a negatively charged redox partner is likely to take place. Our dipole moment compares favorably with the dipole of 308 D calculated by Koppenol and Margoliash using a slightly more simplified electrostatic model involving only formally charged atoms and effective helix dipoles. Their dipole direction is shifted 30° from our best model, and it makes a 43° angle relative to the CH_δ atom along the exposed heme edge (see Figure 1). Surprisingly, the simplified electrostatic models placing only formal charges at actual side chain locations or net residue charges on C_α positions give a reasonably accurate picture of the global electrostatic properties of CYTC relative to the all-atom model.

The computed electrostatic properties of yeast CYP presented here are novel results. The large −12e monopole with undissociated heme propionates is consistent with the observed rapid association kinetics in the reaction with CYTC ($k \approx 10^8$ M^{-1} s^{-1}). But particularly noteworthy is the very large dipole magnitude of 425 D, the *negative* end of which is reasonably correlated with the proposed site of electron transfer with CYTC and other physiological redox partners. The negative axis of the dipole, which will be attracted to the positive monopole and positive dipole end of CYTC, crosses the protein surface approximately at the carbonyl oxygen of Gly-178 in close proximity to a region bounded by aspartates 37 and 79 and asparagine 216, which surround the heme surface edge and are hypothesized by Poulos and Kraut[22] to play

(31) Gupta, R. K.; Koenig, S. H. *Biochem. Biophys. Res. Commun.* **1971**, *45*, 1134.
(32) Moore, G. R.; Williams, R. J. P. *Eur. J. Biochem.* **1980**, *103*, 533.
(33) Hol, W. G. L. *Prog. Biophys. Mol. Biol.* **1985**, *45*, 149.

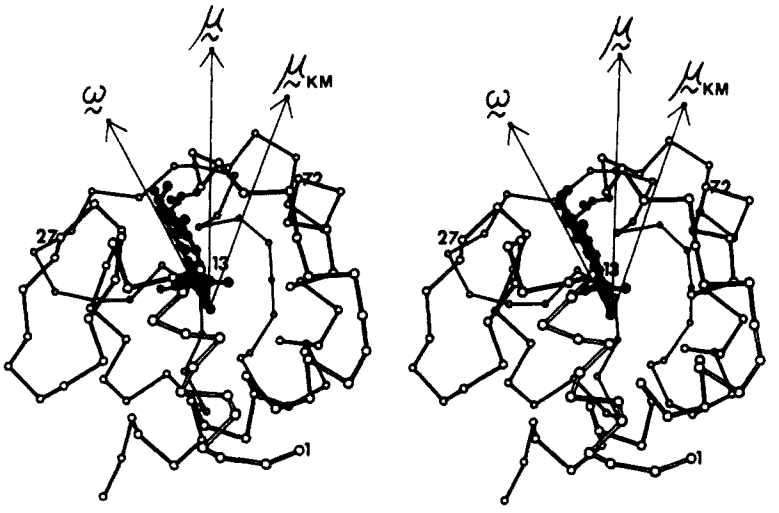

Figure 1. Stereoscopic projection of the C_α skeleton and heme atoms of CYTC depicting the position of the computed dipole moment vector μ relative to a vector ω passing through the exposed heme edge and the dipole vector μ_{KM} predicted by Koppenol and Margoliash.[21] Lysines 13, 27, and 72 important in charge complementarity are indicated.

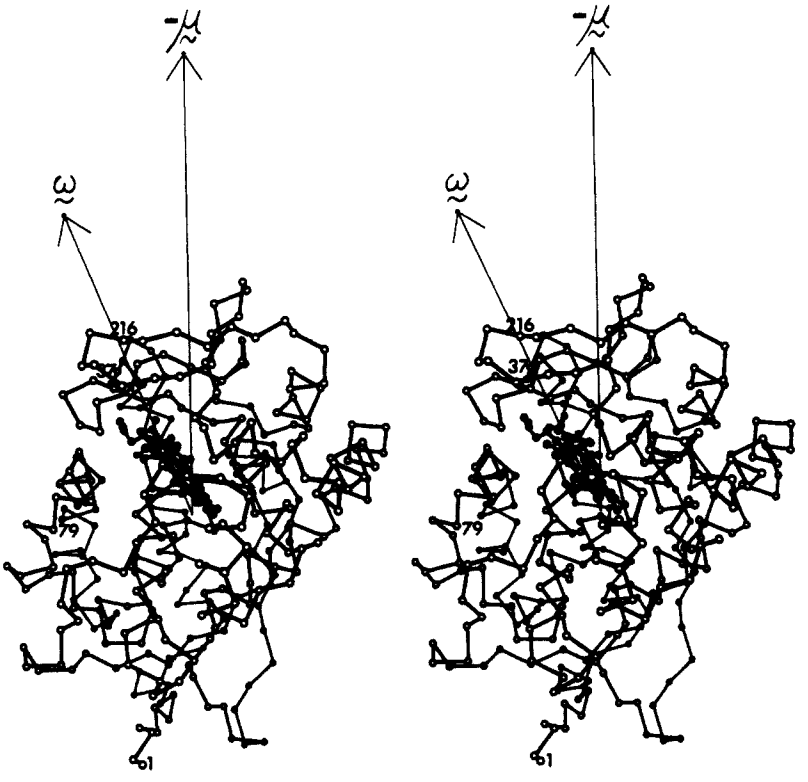

Figure 2. Stereoscopic projection of the C_α skeleton and heme atoms of CYP depicting the position of the computed negative dipole moment vector $-\mu$ relative to a vector ω passing through the exposed heme edge.

a role in the electron-transfer complex with CYTC by showing complementarity with lysines 13, 27, and 72 on CYTC (see Figures 1 and 2).

B. Simplified Model System for Brownian Calculations. For the purposes of computational facility in initial Brownian dynamics simulation studies of association rates of CYTC and CYP described below, it is desirable to adopt a somewhat simplified model of these proteins based on the electrostatic results discussed above. It will be seen that even for the simple model studied here, large amounts of computation time are still required to generate rate constants. We model both proteins as charged spheres having a centrally imbedded monopolar charge carrying the net protein charge and two dipolar charges imbedded 1.0 Å inside the protein surface, with magnitudes computed to generate the dipole moments calculated above. Since the proteins are somewhat elliptical in shape rather than spherical, the estimation of effective radius is somewhat arbitrary. Thus we chose to look at two different system models (model I and model II) which differ in the protein radii and all other parameters which depend directly on radius. Table III summarizes the model parameters for each protein in the two different models. The model I radii R_i of 14 and 21 Å for CYTC and CYP, respectively, are chosen to satisfy the criteria that (a) CYP and CYTC are essentially at closest approach at 35-Å separation (= 14 + 21) with heme regions aligned for electron transfer (this distance has been determined by molecular graphics coupled with empirical energy analysis) and (b) *ratio* of protein sizes corresponds to atom density plots vs. distance from center of mass. Model II radii (18 and 28 Å) were independently estimated purely by examining plots of atom number density vs. distance from the protein center of mass[34] without cognizance of the reaction distance summation criterion noted above.

(34) Boles, J. O., Thesis, in preparation.
(35) Solc, K.; Stockmayer, W. H. *Int. J. Chem. Kinet.* **1973**, *5*, 733.

Table III. Protein Parameters for the Two System Models Employed in the BD Simulations

parameter	model I		model II	
	CYP	CYTC	CYP	CYTC
protein radius (Å)	21	14	28	18
reaction radius (Å)	35		46	
D_T (Å^2/ps)	1.04×10^{-3}	1.54×10^{-3}	7.78×10^{-4}	1.20×10^{-3}
D_R (ps^{-1})	1.76×10^{-6}	5.9×10^{-6}	7.45×10^{-7}	2.78×10^{-6}
monopole charge	−12e	+8e	−12e	+8e
dipole charges	±2.21e	±2.29e	±1.638e	±1.744e
dipole magnitude (D)	425	286	425	286
reactive patch angle θ, deg	10	10	10	10

The translational diffusion coefficient D_{Ti} for each protein is assumed for simplicity to be separation-distance-independent and related to the protein radius R_i by the Stokes–Einstein relationship

$$D_{Ti} = k_B T / 6\pi\eta R_i \quad (1)$$

where $k_B T$ is Boltzmann's constant times absolute temperature. Values in Table III are for water at 25 °C, with a viscosity of $\eta = 1.0$ cP. Rotational and translational diffusion are assumed to be uncoupled for this simulation study. Rotational diffusion constants for each protein are estimated with use of the equation for spherical particles

$$D_{Ri} = k_B T / 8\pi\eta R_i^3 \quad (2)$$

resulting in numerical values shown in Table III.

The proteins are assumed to react only when they achieve a collisional separation distance $R = R_{cyp} + R_{cytc}$ (e.g., 35 Å in model I). Further, they are required to be in a proper orientation for reaction. Each protein is assumed to be anisotropically reactive, having a reactive patch of angle extent θ_i axially symmetric around an orientation vector ω_i as shown in Figure 3. This model system is similar to the classic model of Solc and Stockmayer with the exception that *both* reactive particles have asymmetric reactivity. The angle size θ of the electron-transfer surface on cytochrome proteins is an unknown quantity and is chosen here based upon an estimate of Stellwagen,[34] who estimates a fractional surface area for heme exposure equal to 0.006 in CYTC; this corresponds to a reactive patch angle of $\theta_{cytc} \simeq 10°$.

The electrostatic field effects in the diffusional association rate are treated in this study in an approximate fashion for computational facility. The electrostatic field in the system is generated by assigning three charges to each protein, a monopole and two dipole charges. Monopole charges of +8e and −12e for CYTC and CYP are placed at the centers of the two spheres. Dipole charges are placed at opposite ends of the dipole axis at 1.0 Å inside the surface of the proteins. This placement provides for an ion exclusion radius and thus prohibits singularities in the electrostatic potential when proteins collide along dipole vectors. The dipole magnitudes of 286 and 425 D determined in the best electrostatic model above are generated by assigning dipole charges at these positions of ±2.29e and ±2.21e for CYTC and CYP, respectively, for model I. Simulations were performed with and without dipole force terms to assess the relative effects of electrostatic features of the model. The choice of surface charges rather than a centrally located point dipole of the same magnitude is made (a) to qualitatively reflect the fact that most charged groups on proteins are near the surface and (b) to correspond to our recent finding that the local charge density near the reactive site is more significant in diffusional reaction dynamics of dipoles than global electrostatic features.[14]

The remaining parameter in the protein models to be discussed is the angle γ that the dipole vector μ makes with the orientation vector ω of the reactive surface.[14] This is difficult to determine without knowing the exact structure of the electron transfer encounter complex between the proteins.[22] For example, it would not necessarily be correct to use the angle between μ and the position vectors of heme atoms most clearly exposed at the protein surface, as determined in the previous section, since the most

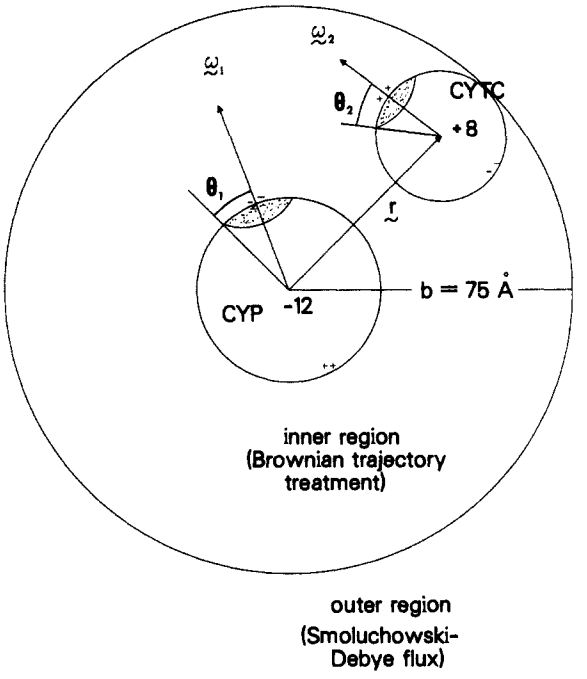

Figure 3. Schematic picture of the simplified model system used in the Brownian simulations in which two proteins (CYTC and CYP) are modelled as spheres each possessing a central monopole carrying the net charge, two dipolar charges near the surface of the protein, and a reactive surface patch of angle extent θ which is axially symmetric about orientation vectors ω.

favorable heme mutual alignment in docked proteins may not necessarily be such that surface heme atoms are at their shortest separation. The reaction criterion may in fact be more complicated. As an initial approximation we will make the assumption that the dipole axes are in perfect alignment with the centers of the reaction surfaces, the positive end for CYTC and the negative end for CYP.

C. Solvent Medium. The solvent medium is water at 25 °C, here treated as a dielectric continuum with a constant dielectric $\epsilon = 78.5$ in the ensuing simulations. For the purposes of these simplified model studies it would be superfluous as well as computationally expensive to attempt to incorporate the discontinuity in the dielectric constant across the protein–solvent interface, although for future studies it is clearly an important goal to use more accurate treatments of electrostatic fields around charged macromolecules in solvent media.[37] We include ionic strength effects using a Debye–Hückel screening term in the electrostatic potential energy equation

$$W = \sum_i \sum_j \frac{q_i q_j \exp(-\kappa(r_{ij} - B_{ij}))}{\epsilon r_{ij}} \quad (3)$$

where summations i and j are over charges on proteins 1 and 2, q_i is electrostatic charge of charge i, r_{ij} is the separation distance between charge i and j, $\kappa = 0.329 I^{1/2}$ is the Debye–Hückel screening parameter in units Å^{-1}, I is ionic strength, and B_{ij} is a

(36) Stellwagen, E. *Nature (London)* **1978**, *275*, 73.

(37) Warshel, A.; Russell, S. T. *Q. Rev. Biophys.* **1984**, *17*, 283.

distance shifting factor for charge i,j interaction included to account for finite size of ions. In order to compare with experimental results for association rates of CYP and CYTC gathered by Kang et al.,[18] simulations were performed with binary monovalent electrolyte ionic strengths $I = 0.1$, 0.16, and 0.25 m, corresponding to κ values of 0.1041, 0.1316, and 0.1645 Å^{-1}. The finite ion size (FIS) correction B_{ij} is found to be extremely important in the simulations, since large molecules are being treated. For instance, a monopolar charge at the center of a protein will not build up an atmosphere of diffusible ions inside the protein, such that the excluded volume of the protein will diminish the screening distance in charge interaction i,j by an amount B_{ij}. In this model the B_{ij} term for the interaction between the two monopole charges at the centers of the proteins is taken to be the sum of the radii of the proteins. At contact separation the monopole–monopole Coulombic interaction term is at full strength. For the interaction between a central monopole charge and one of the surface dipole charges on the other protein, B_{ij} is taken to be the protein radius plus the 1.0 Å imbedding distance of the surface charge, while for the interaction between two surface charges on different proteins $B_{ij} = 2.0$ Å. Obviously, this scheme has a number of deficiencies. First, the electrolyte solution can still mediate and diminish the Coulombic interactions even at protein contact, since screening depends on more than simply the amount of medium along a direct line between the charges. Second, the Debye–Hückel screening term assumes a radially symmetric distribution of ions around a given screened charge, which will not pertain to protein surface charges. Also, proteins in proximity to one another will mutually perturb the ion atmosphere around themselves. As one can see this solvent model is fairly crude and nonrigorous, and clearly it must be improved upon in more detailed studies. However, it will serve here to demonstrate the sensitivity of simulated rate constants to solvent-mediation effects.

D. Brownian Dynamics Simulations. The basic Brownian Dynamics (BD) trajectory simulation method[6] and its extensions[10,11] have been previously described, so we simply provide a sketch. In BD the trajectory of a reactive pair undergoing translational and rotational diffusion in a viscous medium is simulated stochastically by a series of small random displacements chosen from a distribution which is the short time solution of the Smoluchowski equation.[7] If the separation vector in a 2-particle system at time t is $\mathbf{r}(t)$, its value after a time step of duration δt in the absence of reactive or reflecting boundaries is given by the algorithm

$$\mathbf{r}(t + \delta t) = \mathbf{r}(t) + \delta t(k_b T)^{-1} D\mathbf{F} + \mathbf{S} \tag{4}$$

where $\mathbf{F}$ is the systematic direct force acting between the particles at the beginning of the time step, and random force component $\mathbf{S}$ is a vector of Gaussian random numbers of zero mean and variance–covariance satisfying the relationship

$$\langle S_i S_j \rangle = 2D_T \delta_{ij} \delta t \tag{5}$$

Here, D_T is the diffusion constant for relative translational motion between the two proteins in the absence of hydrodynamic interactions and is given by the sum of the individual protein self-diffusion constants as selected above. Northrup et al.[11] have incorporated more accurate algorithms (replacing eq 4) for particle displacements near absorbing and reflecting boundaries, thereby allowing larger time steps to be chosen than are permitted using a free diffusion algorithm near a boundary.

Similar equations exist for the rotational Brownian motion of each particle,[38] where forces in eq 4 are replaced by torques $\mathbf{T}$ and random vector $\mathbf{S}_R$ involves the rotational diffusion coefficients. The equation for the motion of the protein orientation vectors ω_i due to independent rotation is

$$\omega_i(t + \delta t) = \omega_i(t) + \delta t(k_b T)^{-1} D_R \mathbf{T} + \mathbf{S}_R \tag{6}$$

by analogy with eq 4. This simulation is the first of the kind in which *two* reactive asymmetric particles undergo Brownian rotation, each rotating under the influence of torques. Since both particles are macromolecules and are of comparable size, each has a comparable rotational relaxation time which is also on the time scale of translational diffusional relaxation, and so rotational dynamics contributes strongly to the resulting rate calculation. More quantitatively accurate results should be obtained in future studies which include the hydrodynamic coupling between rotational and translational diffusion.[38]

Simulation of a large number of trajectories (5000 for each of the cases studied) is used to calculate the probability $p(b)$ for the reactive encounter of a particle pair starting its diffusion at randomly selected orientations at fixed separation distance b = 75 Å. (The validity of a 75 Å starting surface was tested in independent simulations in which we ascertained that arrivals at this surface starting from randomly generated points on the 200 Å surface were essentially orientation-independent in distribution. That force anisotropies do not extend further into the medium is due to the Coulombic screening at $I \geq 0.1$.) Truncation of unsuccessful trajectories is performed at separation surface c = 200 Å, and an exact truncation correction is applied as described in ref 6. Reaction occurs when protein separation equals collisional separation $R = R_{cytc} + R_{cyp}$, and both orientational reaction criteria

$$\omega_1 \cdot \mathbf{r} > |\omega_1||\mathbf{r}| \cos \theta_1 \tag{7a}$$

and

$$\omega_2 \cdot \mathbf{r} > |\omega_2||\mathbf{r}| \cos \theta_2 \tag{7b}$$

are simultaneously met (see Figure 3), where θ_1 and θ_2 both equal 10°. Since b is chosen such that forces are essentially centrosymmetric beyond b, the steady state diffusional rate constant $k_D(b)$ of first attainment of the spherical surface b from infinite separation is angle-independent (verified here by separate simulation study) and may be calculated by simple Smoluchowski–Debye theory[4,5,39]

$$k_D(b) = \left[\int_b^\infty dr \exp(\beta V(r)) / 4\pi r^2 D_T \right]^{-1} \tag{8}$$

where $V(r)$ is the centrosymmetric (beyond b) interaction free energy, and $\beta = (k_B T)^{-1}$. These quantities may then be combined to obtain exactly the standard bimolecular diffusion controlled rate constant k according to the equation

$$k = k_D(b) p(b) \tag{9}$$

Diffusional rate constant results in this work symbolized with the asterisk superscript are dimensionless rate constants

$$k^* = k / 4\pi R D_T = k / k^\circ \tag{10}$$

where the simulated bimolecular rate constant is scaled by the primitive association rate constant $k^\circ = 4\pi R D_T$ given by the simple Smoluchowski theory[4] for reaction of two neutral isotropically reactive spherical particles reacting at separation R.

III. Simulation Results

A. The Neutral Protein Result. In order to verify the accuracy of the BD method by comparison with existing exact and approximate analytical results, we first treat several simple systems in which no interparticle forces other than excluded volume are present. We first consider the Solc and Stockmayer model[35] where only *one* of the proteins has asymmetric reactivity and is able to rotate on the time scale of translational diffusion while the other protein has uniform reactivity over its entire surface. We compare simulation results to the approximate analytical result of Shoup et al.[40] which virtually exactly reproduces the numerical results of Solc and Stockmayer. Rate constant values for this case with various reactive patch sizes are compared in the upper section of Table IV. Excellent agreement is obtained between the two methods, as expected. Essentially exact agreement is to be expected, in fact, given a sufficiently large number of trajectories and sufficiently small BD time step size.

(38) Dickinson, E. *Chem. Soc. Rev.* **1985**, *14*, 421.

(39) Northrup, S. H.; Hynes, J. T. *J. Chem. Phys.* **1979**, *71*, 871.
(40) Shoup, D.; Lipari, G.; Szabo, A. *Biophys. J.* **1981**, *36*, 697.

Table IV. Comparison of BD Simulation and Analytical-Theoretical Results for Dimensionless Association Rate Constants when Forces Are Absent[a]

model	θ_{cyp}	θ_{cytc}	k^*(BD)	k^*(anal)
I	10	180	0.08	0.08
I	180	10	0.11	0.12
I	30	180	0.27	0.275
I	180	30	0.34	0.34
I	60	180	0.55	0.55
I	180	90	0.82	0.79
II	10	180	0.077	0.08
II	180	10	0.11	0.12
II	30	180	0.27	0.275
II	180	30	0.34	0.34
II	90	180	0.55	0.55
II	180	90	0.82	0.79
I	10	10	0.0008	0.00133
I	30	30	0.041	0.036
I	60	60	0.275	0.287
II	10	10	0.0013	0.00133
II	30	30	0.042	0.0359
II	60	60	0.274	0.287

[a] Proteins are rotating with rotation constants given in section II. Various reactive patch sizes θ_α are considered. Uncertainties in BD results are ±0.01 in upper portion, and ±0.001 in lower portion. k^*(anal) in upper portion are results of Solc and Stockmayer[35] (one reactant particle is isotropic). k^*(anal) in lower portion is approximate analytical result given by eq 11 (when both particles are anisotropically reactive).

The analytically intractable case in which *both* particles are asymmetrically reactive and are able to rotate can also be easily obtained by BD simulation. Reference to several treatments of this situation has been given in the excellent recent review by Berg and von Hippel.[3] For reactive patches that are small compared to the molecular dimensions of the interacting particles, such that the duration of an encounter is small compared to the rotation time required to orient into a productive complex, a useful approximate relationship based on geometric arguments is[41]

$$k \simeq k^{\circ}\theta_1\theta_2(\theta_1 + \theta_2)/8 \qquad (11)$$

A comparison of BD results to eq 11 predictions in the lower portion of Table IV shows surprisingly good agreement, even for the 60° patch size trial which violates the spirit of the approximation required to obtain eq 11. Note that the double constraint on reaction when both particles must be in a special orientation has a drastically retarding effect on the rate constant. When both proteins have patch sizes of 10°, which perhaps most closely corresponds to the CYTC–CYP reaction, the rate constant is three orders of magnitude smaller than the Smoluchowski limiting rate constant for isotropic neutral particles with no orientational constraints. Substituting the appropriate values of D_T and R and converting to units of L/(mol·s), the $(\theta_{cyp},\theta_{cytc}) = (10°,10°)$ case in the absence of forces yields a bimolecular association rate constant of 5×10^5 M^{-1} s^{-1} for model I, compared to the observed rate constant for CYTC–CYP association[16] near 10^8 M^{-1} s^{-1} (see Figure 4). Not surprisingly, the electrostatic interactions must play a dominant role in overcoming the three-orders-of-magnitude retarding effect of the severe geometric constraints present in the CYP–CYTC association reaction. This will be demonstrated in the context of the simple electrostatic charge model in what follows.

B. Diffusional Rate Constants for the Electrostatic Models. Simulation results in the presence of electrostatic forces are shown in Table V for various models and are compared with experiment in Figure 4. Runs are generated primarily for ionic strengths greater than or equal to 0.1 m, since only in this regime is the diffusional association event rate-limiting, and we may compare our results directly with kinetic studies of Kang et al.[18] At low ionic strength, the experiment shows that the electron-transfer reaction is limited by the *dissociation* rate of the complex rather

(41) Schurr, J. M.; Schmitz, K. S. *J. Phys. Chem.* **1976**, *80*, 1934.

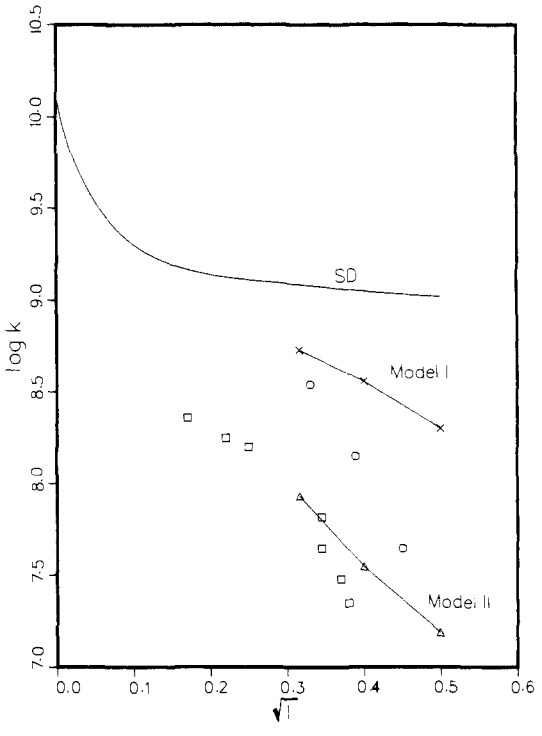

Figure 4. Brønsted–Bjerrum plot of log of the diffusion-controlled bimolecular rate constant for CYTC–CYP association vs. square root of ionic strength. Experimental results of Kang et al.[18] in chloride (○) and phosphate (□) buffers are compared with a primitive SD treatment for isotropically reactive monopolar charged proteins, and two Brownian-dynamics-simulated realistic monopole/dipole models (of different protein radii) with orientational constraints to reaction.

than the diffusional association step. Thus, in the dissociation-limited regime the overall rate process speeds up as ionic strength increases until the optimal ionic strength is reached. In the BD simulation for ionic strengths much less than 0.1 m, the proteins are entrapped at an encounter separation sufficiently long by the strong +8e ... −12e monopolar Coulombic attraction that the reaction partners may explore their entire orientation space by rotational diffusion, and reaction occurs essentially at every encounter. In such cases, the dipolar charges and asymmetric reactivity of the model system are irrelevant, and diffusional association rate constants may be computed by simple Smoluchowski–Debye theory for orientationally nonspecific encounter rate without doing BD simulation (eq 8 with b replaced by collision separation R). For example, in model I at zero ionic strength a rate constant $k^* = 20.04$ (20 times larger than the primitive Smoluchowski result for neutral spheres) or $k = 1.2 \times 10^{10}$ M^{-1} s^{-1} is obtained by numerical integration of eq 8.

The diffusional rate constant is significantly slower at ionic strength 0.1 m and also shows dependency on the model features such as dipole forces, reactive patch sizes and orientations, and electrolyte solution treatment, indicating that rotational motion and electrostatic torques are important. In Table V we may note that (at fixed reactive patch sizes equal to 10° on both proteins) two factors emerge as being clearly significant: (i) the inclusion of dipolar steering forces and (ii) inclusion of finite ion size (FIS) effects in the Debye–Hückel screening model utilized. Using only monopolar charges on each protein and a primitive DH screening model (all $B_{ij} = 0$; no finite ion size provision), we obtain a diffusional rate constant $k = 1.2 \times 10^6$ M^{-1} s^{-1} for model I, which is two powers of ten smaller than the range of experimental rate constants. The reaction rate is significantly enhanced by the inclusion of dipolar surface charges on each protein which lie along the patch orientation vector such that the positive end of the CYTC dipole is at the reactive patch of CYTC and the negative end of the CYP dipole is at the reactive patch of CYP. These dipolar charges give rise to torques which rotate encountered proteins into favorable orientation for reaction and enhance the rate by a factor

Table V. Diffusional Association Rate Constants for the CYP–CYTC Reaction Computed by BD Simulation Using Model I and Various Electrostatic Terms and Solvent Treatments

case						
cyp:cytc interaction[a]	solvent treatment	I	θ_{cyp}	θ_{cytc}	k^*(BD)	k(BD), M^{-1} s^{-1}
no charges			10	10	~0.0008	$\sim 5 \times 10^5$
MD:MD		0.0	10	10	20.0	1.2×10^{10}
M:M	DH	0.1	10	10	0.0020	1.2×10^6
MD:MD	DH	0.1	10	10	0.023	1.4×10^7
MD:MD	DH with FIS	0.1	10	10	0.893	5.4×10^8
MD:MD	DH with FIS	0.16	10	10	0.601	3.6×10^8
MD:MD	DH with FIS	0.25	10	10	0.333	2.0×10^8

[a] M:M = monopole:monopole interaction only. MD:MD = monopole/dipole:monopole/dipole interaction. DH = for Debye–Hückel screening law treatment of ionic strength effects. FIS = for finite ion size correction in DH screening law.

of 10 to 1.4×10^7 M^{-1} s^{-1} for model I, but this is still at least a power of ten smaller than experimental results. Clearly, other factors must be considered in the electrostatic model in order to account for the considerably faster rates observed in the experiment ($\sim 10^8$ M^{-1} s^{-1}). Inclusion of finite ion size effects for all charge interactions into the DH treatment enhanced the rate by an additional factor of 40 to a value of $k = 5.4 \times 10^8$ M^{-1} s^{-1} for model I. This dramatic enhancement is clearly a result of dipolar steering that the large −12e monopole of CYP exerts on the positive end of the CYTC dipole vector and the +8e monopole of CYTC exerts on the negative end of the CYP dipole vector. The attractions between surface charges themselves seem to play a less important role. Note that the rate constant in this model is finally in reasonable agreement with the experimental results in the chloride buffer as we can see in Figure 4. Model I predicts a rate which is slightly larger than the experiment (chloride buffer), while in model II, in which the protein radii are somewhat larger, the theoretical rate falls below the experimental rate in chloride buffer but is similar to the result in the phosphate buffer. The smaller proteins in model I, despite a smaller target for reaction than model II, react faster primarily due to the more rapid rotational search relative to the time duration of protein encounters. For example, in the $I = 0.1$ m, DH/FIS case, 70% of all encounters are followed by reorientation and reaction in model I, whereas the fraction is only 12% in model II. The rates of nonstereospecific encounters in model I and model II are virtually the same ($k = 7.7 \times 10^8$ and 7.4×10^8 M^{-1} s^{-1}, respectively). The smaller experimental rates for the phosphate buffer are perhaps due to more substantial ion site-binding which negates the effectiveness of surface charges in steering molecules into productive encounter orientations, a feature which is entirely neglected in our study.

Both the experimental and BD-simulated rate constants show a dependency on the ionic strength of the medium, as exemplified in the Brønsted–Bjerrum plot in Figure 4, but the experimental dependency is somewhat greater. Linear dependence of log k vs. $I^{1/2}$ predicted by the Brønsted–Bjerrum equation for reaction rate constant of charges q_a and q_b

$$\log k = \log k_{I=0} + 1.02 q_a q_b I^{1/2} \qquad (12)$$

is observed to some extent by the experimental results, but with effective charge product value for $q_a q_b$ of only −7.5 in the chloride buffer, which is substantially smaller than what one would expect based on the charges of these molecules. In actuality, one does not expect the Brønsted–Bjerrum relationship to hold at all in this reaction for a variety of reasons: (i) the Debye–Hückel theory is valid at low I but becomes a poorer approximation at ionic strengths studied here, particularly for such large net charges where the intermolecular potential energy is well in excess of $k_B T$, (ii) eq 12 is derived under the assumption that no ionic complexes form between the proteins and electrolyte ions (no site-binding), (iii) the proteins are not spherically isotropic monopoles but have a more complicated charge distribution, and (iv) the derivation of eq 12 is based on the activated complex theory of chemical reactions, and is thus not valid in the diffusional limit. The top curve in Figure 4 is the rate constant predicted by the Smoluchowski–Debye theory for isotropically reactive monopolar-charged particles of charges −12e and +8e and shows behavior which is far from linear and has a slope significantly smaller than what the Brønsted–Bjerrum relation predicts for a −12e,+8e ion pair. Yet the Smoluchowski–Debye theory is itself consistent with all of the assumptions used to obtain eq 12 except a most important one, and that is item (iv) above. Thus, we emphatically state that, despite its use in the literature, it is clearly inappropriate to correlate *diffusion-controlled* rate data using a Brønsted–Bjerrum relationship. The slopes of the BD-simulated rate constant curves for models I and II are somewhat less negative than the experimental curves and give quantitative agreement only in a small ionic strength window near physiological ionic strength (~0.1 m). This lack of adherence to the experimentally observed ionic strength dependence as ionic strength increases is primarily due to the lack of validity of the screened Debye–Hückel Coulombic potentials and an absence of consideration of site-binding effects in our model. Several other explanations may be advanced for our lack of perfect quantitative agreement. The overall charge of the proteins may be improperly estimated when assuming the state of protonation of basic and acidic amino acid residues. We include no discontinuity in the dielectric constant across the protein–solvent interfaces. A highly simplified charge distribution on the proteins has been assumed in treating proteins as simple dipoles. We totally ignore the effect of irregular surface topography of real proteins and the hydrodynamic coupling effect. However, the poor agreement with experiment without electrostatic enhancement or with only monopolar interactions and the reasonable agreement with the inclusion of the dipole terms is encouraging, and it demonstrates beyond doubt the importance of details of electrostatics in the dynamics of this electron-transfer process. For example, at the outset of this study it was not obvious whether details of the charge distribution would have an effect on the rate, since the strong attractive monopolar interactions might be expected to dwarf more subtle details of molecular architecture. The simulation appears to produce good agreement when ionic strength is large enough that diffusional association is rate limiting and small enough that the treatment of solvent mediation effects with simple continuum dielectric models is adequate.

C. The Effect of Electrostatic Torque on Reaction Dynamics. An important aspect of diffusional macromolecular interactions is the well-known effect of reduction in dimensionality. It has been argued that biological systems make extensive use of the principle that reactant particles are effectively trapped on lower dimensional surfaces of their relative configuration space and can then more effectively explore this subspace until reaction occurs. This behavior may apply to small molecules confined by intermolecular forces and sliding along DNA and reacting with specific nucleotide sequences or to molecules nonspecifically attached to membrane surfaces and ultimately reacting with membrane-bound partners. In a certain sense such behavior is observed in the case simulated here. The long-ranged Coulombic attractive forces not only extend the effective capture radius for the encounter of the two proteins but also serve to entrap the pair at small separations until the dipole-generated torques can rotate the proteins into favorable orientation for reaction. The relationship between the duration of Coulombic entrapment of encountered particles and the time required for the interactants to seek out the correct mutual orientation is of extreme importance in the overall dynamics of the reaction. For this reason an independent BD simulation was

Table VI. Results for Independent BD Simulations Computing Average Times of Relevant Processes in the Translation–Rotational Diffusional Reaction of CYTC and CYP Proteins[a]

process	mean time (10^6 ps) model I	model II
Coulombic entrapment	1.8	0.10
reorientation and reaction of entrapped proteins in presence of dipolar steering torques	0.40	3.7
reorientation and reaction of entrapped proteins in absence of dipolar steering torques	17.3	56.5

[a] The case is $I = 0.1$ m, DH screening with finite ion size corrections on all interactions, full monopole/dipole charge distribution on both proteins.

performed to determine the relative times for the dissociation and orientational processes. The average *Coulombic entrappment time* due to the monopolar attractive force was calculated for the case at $I = 0.1$ *m* with DH screening and FIS effects. The entrapment event is defined to begin for model I (II) when proteins achieve separation of 40 (50) Å and to end when particles escape to 50 (60) Å radius. These surfaces are separated to avoid counting rapid infinitesimal surface recrossings at any given surface. Multiple repeated entrapments may occur before actual reaction event (1.3 is the average number of encounters per trajectory observed in model I for trajectories in which an encounter occurred). The duration of such encounters is to be compared to the average time required for encountered pairs to achieve the correct mutual orientation for reaction. This average was calculated in a separate simulation in which the proteins were constrained to translationally diffuse on an interparticle separation surface at the collision separation (35 Å) with full rotational freedom and torques acting. Trajectories were begun at random points on this surface and with proteins at random orientations. The mean first passage time to achieve reactive orientation was then computed for 50 trajectories. An identical simulation was performed in the total absence of any Coulombic steering torques. The results of these simulations are shown in Table VI. Note that in model I the time required to reorient the proteins in the presence of steering torques is an order of magnitude less than the time the particles are held in proximity by monopolar attractive forces. This provides an explanation for the fact that the rate constant for the highly constrained $(\theta_{cytc},\theta_{cyp}) = (10°,10°)$ case ($k = 5.4 \times 10^8$ M^{-1} s^{-1}) is nearly (70%) as large as the rate constant of isotropically reactive proteins $(\theta_{cytc},\theta_{cyp}) = (180°,180°)$ ($k = 7.7 \times 10^8$ M^{-1} s^{-1}). Without the steering torques, an exceedingly long time is required for proteins to search their mutual orientation space and react (17.6×10^6 ps), resulting in a drastic retardation of the rate when orientational constraints to reaction are applied in the absence of dipolar torques ($k = 1.2 \times 10^5$ M^{-1} s^{-1}).

IV. Summary and Conclusions

In this paper the BD method has been applied to calculate the diffusion-controlled association rate of electron transfer proteins cytochrome *c* and cytochrome *c* peroxidase. Each protein is modelled as a sphere having a centrally located monopolar charge and two dipolar surface charges. Charge magnitudes have been determined by computing the monopole and dipole moment of the proteins directly from extensions of the X-ray crystallographic coordinate sets. The dipole moments of both proteins are found to correlate strongly and in an electrostatically favorable manner with their hypothesized electron-transfer sites. By direct comparison with experimental kinetic studies on this system, it is shown that the presence of torques arising from the dipolar terms are of utmost importance in obtaining simulated rate constants in quantitative agreement with experiment. This is the first computation of its kind to simulate rotational behavior of *two* anisotropic reactive molecules subject to mutual torques. The simulation results are also found to be very sensitive to the mode of treatment of solvent mediation effects. For instance, the inclusion of finite ion size corrections into the Debye–Hückel screening law is essential for producing simulation results which agree with experiment. The large Coulombic attractive forces from the monopole terms of the potential serve to entrap the proteins for a sufficient duration that, when dipolar terms are present, the proteins have the opportunity to explore their orientation space until reaction may occur. Thus we see what amounts to a reduction in dimensionality at least partially operating. Nevertheless, the dipolar terms are essential to steer the proteins into productive orientations during encounters. Ionic strength dependence of the rate constant beyond physiological ionic strength is not well reproduced by the theory. We believe this stems from the inadequate and nonrigorous treatment of solvent mediation effects by a simple continuum screened Debye–Hückel potential. For instance, we ignore the effects of diffusible ions which may bind at specific sites on the protein surface and thus moderate their influence.

Although this study is only very preliminary, the obvious model sensitivity of the results demonstrates the need to carefully consider the electrostatic charge distribution and have an accurate model for solvent mediation effects in order to make quantitative comparisons with experiments and thereby gain an understanding of the diffusional reaction dynamics of biomolecules. Though the model system studied here is obviously oversimplified, a large amount of computation time was still required to generate the results presented (a total of ≈200 h of Vax 11/780 processor time was required). Therefore this study has laid important groundwork for more accurate model studies which will undoubtedly require the use of supercomputers. In order to obtain perfect quantitative agreement, a number of deficiencies of the present simplified model must be removed. The Debye–Hückel screened Coulombic potential must be replaced by a more accurate theory to adequately treat ionic strength effects. The overall charge of the proteins may be improperly estimated when assuming the state of protonation of basic and acidic amino acid residues. A highly simplified charge distribution on the proteins has been assumed in treating proteins as simple dipoles. We include no discontinuity in the dielectric constant across the protein–solvent interfaces. Site-binding effects of electrolyte ions, ignored in our calculations, will become increasingly more relevant at higher ionic strengths, which will alter the ionic strength dependence. We totally ignore the effect of irregular surface topography of real proteins and the hydrodynamic coupling effect between rotational and translational degrees of freedom. Improvements in these several features are to be accomplished in future work.

The understanding of the relationship between structure, dynamics, and reactivity of biomolecules is significant not only in the understanding of biological processes but also for more pragmatic purposes such as drug design and the construction of artificial enzymes with preselected specificities.

Acknowledgment. This work has been made possible by Grants AM01403 and GM34248 from the National Institutes of Health and by the donors of the Petroleum Research Fund, administered by the American Chemical Society. The authors express thanks to Wilfred van Gunsteren for kindly making the GROMOS package available, to Steve Harvey, Stu Allison, and Andy McCammon for helpful discussions, and to Paul Nichols, Christine Northrup, Kevin Reinheimer, and Harold Carney for graphics assistance and secretarial support. S.H.N. is the recipient of an NIH Research Career Development Award.